Soft Matter

Accepted Manuscript

ROYAL SOCIETY OF CHEMISTRY

www.rsc.org/softmatter

Hysteretic DC electrowetting by field-induced nano-structurations on polystyrene film

Yogesh B. Sawane[1], Suwarna Datar[2], Satishchandra B. Ogale[3] and Arun G. Banpurkar[1]*

[1]*Centre for Advanced Studies in Condensed Matter and Solid State Physics, Department of Physics, S P Pune University, Pune-411007* (*India*).

[2]*Department of Applied Physics, Defence Institute of Advanced Technology, Girinagar, Pune-411025*(*India*)

[3]*National Chemical Laboratory (CSIR-NCL), Dr. Homi Bhabha Road, Pashan, Pune-411008,* (*India*).

**Email: agb@physics.unipune.ac.in*

Abstract

Electrowetting (EW) offers executive wetting control of conductive liquids on several polymer surfaces. We report a peculiar electrowetting response for aqueous drop on polystyrene (PS) dielectric surface in ambient of silicone oil. After the first direct current (DC) voltage cycle, the droplet failed to regain Young's angle, yielding contact angle hysteresis, close to a value found in ambient *air*. We conjecture that the hysteretic EW response appears from *in situ* surface modification by means of electric field induced water-ion contact with PS surface inducing nano-structuration by electro-hydrodynamic (EHD) instability. The Atomic Force Microscopy confirms the formation of nano-structuration on electrowetted surface. The effects of molecular weight, applied electric field, water conductivity and pH on nano-structuration are studied. Finally, the EW based nano-structuration on PS surface is used for enhanced loading of aqueous dye on hydrophobic surface.

1. Introduction

Polymers are the key materials in recent technology due to their extraordinary properties such as chemical and electrical resistance, transparent to visible radiation and low dielectric constant etc.[1-3] It is used in many strategic research sectors including biosensor, corrosion resistant materials[4] and materials for micro-fluidic and cell cultures.[5] The hydrophobic property of many polymers is widely explored in developing water repellent paints and coatings. Also the wetting of polymer surface can be further changed by altering surface topology and/or surface chemistry. For instance, water repellent surfaces are produced by suitable hierarchical micro-nano surface roughness covered with self assembled monolayer (SAM) or fluoropolymer.[6,7] On the contrary polymer surface when exposed to oxygen plasma[8] or UV radiations[9] shows enhanced wetting of water. These changes in wetting property of the polymers are long lasting.

In contrast, electrowetting[10,11] is a convenient tool for reversible wetting on many dielectric surfaces under the influence of external voltage, applied between the liquid and an electrode underneath the dielectric. The dielectric surfaces are generally polymers with low surface energy possessing high contact angle (CA). Since last two decades there has been a growing demand and uses of EW for various applications such as liquid lenses,[12] video speed displays,[13,14] microfluidic devices and in micro-total analysis systems (μ–TAS).[15]

Polystyrene (PS) is frequently used in making microfluidic devices and biological culture plates[16-18] yet it is rarely used as a dielectric material in the EW based fluidic devices. The usefulness of the polymer coating is mainly decided by the durability to EW and voltage cycles, therefore detailed EW study on PS surface for many voltage cycles in ambient air and in ambient oil is essential. Fig. 1 shows a schematic of generic EW setup consisting of a conductive water droplet placed on flat PS surface and DC voltage is applied between the droplet and the planar electrode buried in the dielectric. The electrical surface energy reduces

effective liquid-solid surface energy thereby increasing the wetting of liquid (decreasing apparent contact angle) on the solid surface. Thus CA, in the presence of external voltage is a function of the ratio of electrical surface energy to surface energy of liquid, given by following Young-Lippmann eqn:[11]

$$\cos\theta(U) = \cos\theta_Y + \frac{C}{2\gamma_{LV}}U^2 \quad \text{-------- (1)}$$

where $\theta(U)$ and θ_Y are voltage dependent contact angle and Young's contact angle respectively. The surface energy between liquid and ambient medium is γ_{LV} and capacitance per unit area is $C = \varepsilon\varepsilon_o/d$, where $\varepsilon\varepsilon_o$ and d are permittivity and thickness of the dielectric medium, respectively.

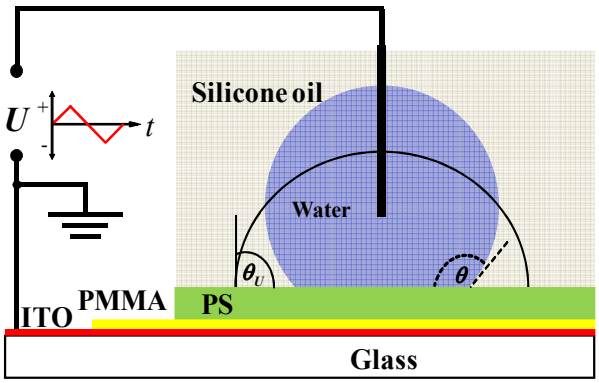

Fig. 1 Schematic shows the setup used for EW on PS dielectric for water droplet in ambient of silicone oil. Poly(methyl methacrylate) (PMMA) buffer layer was used to arrest delamination of PS film in ambient oil.

Bharat Bhushan *et al* [19] have examined the effect of both AC and DC voltage on wetting of water droplet on PS surface in ambient air where contact angle hysteresis (CAH) of 27° for DC voltage and 22° for AC voltages was reported. The reduction in CAH in case of AC field is due to the time dependent electrostatic de-pinning force at the three phase contact line.[20] However, large CAH put significant limitation on usefulness of the dielectric in the practical

applications. Also saturation in contact angle is not yet satisfactorily answered. Several mechanisms have been proposed to explain the saturation in CA such as charge trapping,[21] fluid ionization at the contact line,[22] imperfectness of dielectric,[23] the vanishing solid-liquid interface tension[24] and dielectric breakdown.[25] In general replacing *air* with immiscible *oil* offers several advantages such as less contamination, no evaporation of aqueous liquid and minimal CAH.[26,27] We have investigated EW response on PS dielectric for water droplet in ambient of silicone *oil* and for several voltage cycles. The voltage dependent change for the first voltage cycle shows consistency with Young-Lippmann equation but after removal of external voltage, water droplet failed to regain initial Young's angle. This unusual EW response is analyzed particularly in the light of the electrowetting induced water-ion contact on PS surface rendering surface nano-structuration by electro-hydrodynamic (EHD) instability.

2. Experimental

2.1. Growth of Polystyrene (PS) film

The PS films were grown on conductive Indium Tin Oxide (ITO) glass substrate using solution dip-coating technique. A nanometer thick buffer layer of Poly(methyl methacrylate) (PMMA) was coated prior to polystyrene to improve adhesion of PS on ITO surface in ambient silicone *oil*. The PMMA granules ($\bar{M}_w$ = 98500, Sigma Aldrich) at 10 wt. % concentration were dissolved in Benzene solvent to prepare PMMA solution. Also PS solutions (10 wt. % concentration) were prepared in toluene solvent. PS beads having average molecular weights $\bar{M}_w$=192000 and 35000 were purchased from Sigma Aldrich, USA. The polymer solutions were prepared at room temperature and constantly stirred for more than 6 hours. The homogenous solution was then filtered using syringe filter (PTFE membrane pore size ~ 0.45 μm). This clear solution was used for dip-coating. The commercial ITO glass substrates (purchased from Solaronix) were used as bottom electrodes. These substrates were

cleaned in ultrasonic bath using aqueous detergent solution and subsequently rinsed in distilled-water (DW), acetone, ethanol and finally rinsed in isopropyl alcohol. These substrates were dried in dry nitrogen flow and then PMMA buffer layer was applied at fixed dipping and withdrawal speed of 7 cm/min. This layer was dried in a laminar flow for 10 min and finally cured at 100 °C in a vacuum oven for 6 hours. It was slowly cooled to the room temperature then PS coating was applied using same dipping and withdrawal speed of 7 cm/min and to achieve desired layer thickness, the dip coating is repeated thrice after air drying for 15 min. The substrates were heated at 100 °C for 12 hours in a vacuum oven for final curing and also for removal of solvent and moisture content if any. These substrates were immediately stored in a vacuum desiccator, henceforth referred as pristine PS films. The polymer thickness was estimated using the stylus profiolometer (KLA Tencor P-16+). The PMMA buffer layer thickness was found to be $d_{(PMMA)}$ = 100 nm and polystyrene film thickness was d(PS) = 2.3 ± 0.2 μm. The measurement of CAH on the pristine PS surfaces in ambient air was performed using Advancing Receding Contact Angle (ARCA) technique on the optical contact angle (OCA) goniometer. The volume of water droplet was inflated/deflated at the rate of 3 μl/min using Harvard (Pico Plus) syringe pump and simultaneously advancing/receding contact angle was recorded. Here CAH of 17^{o} was found which is consistent to the result by Bharat Bhushan *et al.*[19]

2.2. Electrowetting on PS surface

Fig. 1 shows a schematic of the EW setup used for DC EW response. The conductivity of distilled water (DW) was increased to 1 mS/cm by adding KCl salt. The water droplet (5 μl) was pipetted on PS surface for EW study. The silicone oil (5 cS, Sigma-Aldrich) was used as an ambient due to several advantages such as nanometer thick lubricating oil layer yielding very low CAH,[28] density matching and arresting water evaporation. We used source meter (Keithley-2400) as a voltage source programmed for the desired voltage ramp as shown in the

schematic Fig. 1. The applied voltage was linearly increased in steps of 2 V with a delay of 0.5 s keeping time rate of change of voltage $dU/dt = 4\ V\ s^{-1}$. The real time contact angle as a function of the voltage magnitude was measured using OCA goniometer system and the experiments were repeated for several voltage cycles on fresh water drop pipetted on pristine polystyrene surface.

2.3. Surface characterization

The surface morphology of the pristine PS surface as well as the electrowetted surface were extensively analyzed using Atomic Force Microscopy (AFM) (MFP-3D from Asylum Research). Attenuated Total Internal Reflectance-Fourier Transform Infrared (ATR-FTIR) spectroscopy (Jasco FT/IR 6100) was used to detect chemical changes in the electrowetted PS surface if any. Also glass transition temperature of PS beads was measured using DTA-TGA analysis (Mettler Toledo TGA/DSC1 star system).

The effective value of the dielectric constant for PMMA-PS bi-layer was determined using the model proposed by Bharat Bhushan *et al.*[19] The capacitance per unit area C_{eq} of the PMMA-PS dielectric is given as

$$C_{eq} = \frac{C_{PS}C_{PMMA}}{C_{PS}+C_{PMMA}}$$

$$C_{eq} = \frac{\left(\frac{\varepsilon_0\varepsilon_{PS}}{d_{PS}}\right)\left(\frac{\varepsilon_0\varepsilon_{PMMA}}{d_{PMMA}}\right)}{\left(\frac{\varepsilon_0\varepsilon_{PS}}{d_{PS}}\right)+\left(\frac{\varepsilon_0\varepsilon_{PMMA}}{d_{PMMA}}\right)}$$

$$C_{eq} = \frac{\varepsilon_0\varepsilon_{PS}\varepsilon_{PMMA}}{\varepsilon_{PS}d_{PMMA}+\varepsilon_{PMMA}d_{PS}} \qquad \ldots(2)$$

The subscript PS and PMMA are used to denote dielectric constant and thickness of the corresponding layer. The capacitance per unit area was determined from of the dielectric thickness measured from profilometer and known dielectric constants. This value was

experimentally verified by fitting Young-Lippmann eqn (1) to the EW response of water droplet using previously estimated value of oil-water interfacial tension $\gamma_{LO} = 38\ \mathrm{mNm^{-1}}$.[29]

3. Results and Discussions

3.1. EW response on PS

The EW response for several periodic voltage cycles on PS surface is shown in Fig. 2 (a). Before EW cycle, water droplet in ambient *oil* shows equilibrium Young angle θ_Y greater than 150°. This CA is significantly large compared to Young angle on bare PS surface in ambient air ($\theta_Y \approx 95^o$). This difference is mainly due to lesser interfacial tension of water-*oil* ($\gamma_{LO} = 38\ \mathrm{mNm^{-1}}$) than interfacial tension of water-*air* ($\gamma_{LV} = 72\ \mathrm{mNm^{-1}}$). The change in CA is plotted against applied voltage to water droplet starting from positive polarity (+U) then reaching to +U_{max} and reverting to negative polarity cycle reaching to (-U_{max}) and finally the cycle completes at U = 0 V. Also the EW response was similar for voltage cycles that begins with negative voltage to the droplet with respect to bottom ITO plate (data not shown). This shows that EW on PS surface is independent to initial voltage polarity on the water droplet. Fig.2 (a) shows that water CA decreases with voltage magnitude but when voltage is reduced to zero, CA increases via different path and reaches to a new Young-angle (θ_{Ynew} ~132°), about 20^o less than the previous one. Thus EW response on the same drop for consecutive voltage cycles starts from this new Young-angle demonstrating large CAH in EW response (see Fig. 2 (a)). We analyzed advancing and receding EW response on PS surface for checking the reliability with Young-Lippmann equation (eqn 1). Fig. 2(b) shows plot of CA against voltage. Also cosine of CA against square of applied voltage (U^2) is shown in the inset. The linear variation in cos θ(U) against U^2 validates Young-Lippmann equation (eqn 1). The slope value of this plot is proportional to dielectric capacitance per unit area which is used to determine effective dielectric constant of bi-layer by substituting value of water-*oil* surface tension $\gamma_{LO} = 38\ \mathrm{mNm^{-1}}$ and total thickness of the dielectric layers

(PMMA+PS). Thus value of effective dielectric constant is ε_{eq}(EW) = 2.56 ± 0.12. Also we determine the value of effective dielectric constant by substituting thickness values and dielectric constants for PS and PMMA [30] in eqn 2 which give ε_{eq}(Model) = 2.54. Both the values of dielectric constants show excellent match conforming Young-Lippmann electrowetting response on PS surface. In the present study, the EW response was deliberately tested well below the CA saturation to prevent charge injection in PS surface and dielectric leakage.

The change in the initial Young angle and apparent hysteresis after the first voltage cycle on PS surface is surprisingly unusual, since ambient *oil* normally provides low CAH. Also, the water droplet attains the new Young angle (θ_{Ynew} ~132°) about 20° below its initial value (θ_Y = 152°). This hysteresis is identical in case of positive and negative voltage polarities to the drop. Also EW response (see Fig. 2 (b)) is symmetric about 0 V. This observation rules out the possibility of electric-field induced charge injection and charge trapping in PS layer.[22]

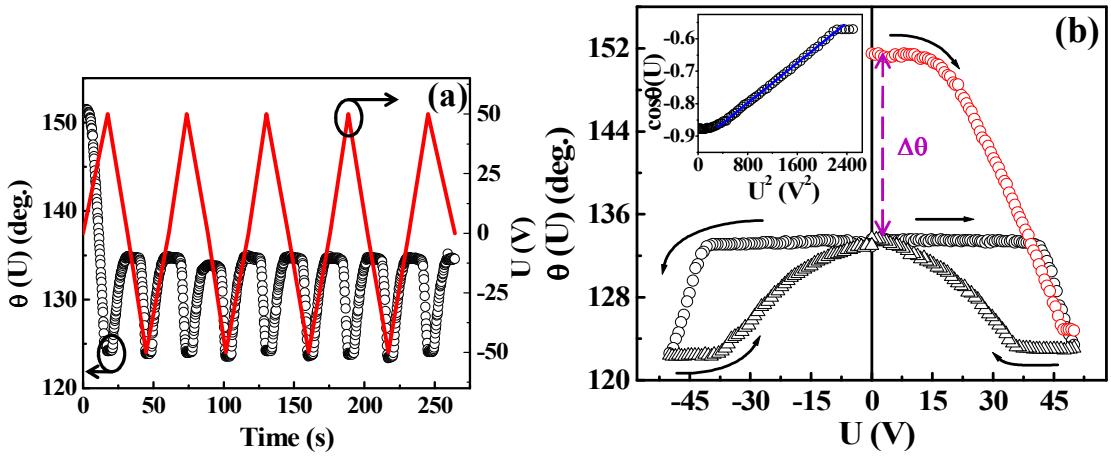

Fig. 2 (a) Variation in the CA (○) of water droplet and the linearly varying voltage amplitude (——) are plotted against time advance. (b) The Electrowetting response plotted as θ(*U*) against the applied voltage begins with positive polarity on droplet. The arrow indicates path of change in CA for increasing and decreasing voltage amplitude. Inset shows cosine of contact angle as a function of voltage square (U^2) for the first voltage cycle. Also least-square linear fit to the experimental data points is shown by a continuous line.

In the past, several models are proposed to explain CAH on the surface. Santos *et al* have proposed that the friction at the triple line decides the dynamic contact angle.[31] Li *et al* have proposed that the contact angle value is based on the local wetting at contact line.[32] Also Extrand *et al* clearly demonstrated using series of experiments that the wetting phenomenon is controlled by the interaction at the contact line.[33] However, Johnson and Dettre were the first to carry out a detailed study related to CAH on the surface with varying roughness.[34] They found that magnitude of hysteresis increases with surface roughness. P. G. de Gennes has discussed several factors for CAH like elasticity of triple line, uncorrelated surface defects etc.[35] Thus to understand the hysteretic EW on polystyrene surface, it is essential to analyze electrowetted surfaces for any surface modification. EW induced dielectric surface modification and associated hysteretic EW response is not yet studied and needs a detailed investigation.

To explore this effect we first studied transient electrowetting response on PS surface at different increasing electric field strength (see Fig. 3). The decrease in the contact angle of water drop with voltage magnitude is clearly seen and above certain critical voltage (electric field), about ~ 50 V in the present case, the drop attains new Young angle $\theta_{Ynew} \approx 140^{o}$ giving partial CA recovery in the subsequent voltage cycles and decrease in CA occurs below this Young angle $\theta_{Ynew} \approx 140^{o}$.

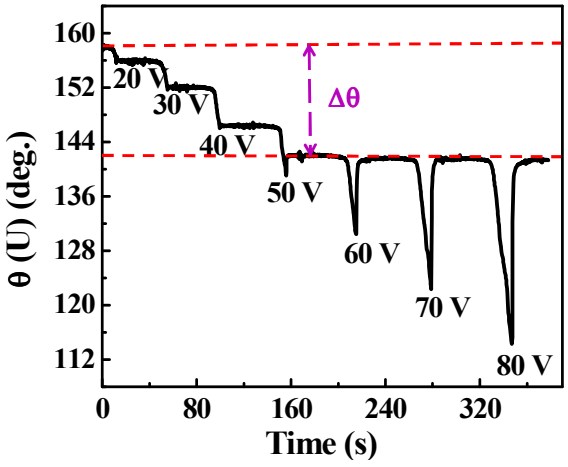

Fig. 3 The variation in electrowetting response (CA change) for pulsed DC voltage (pulse width τ = 1 s) is plotted for increasing voltage magnitude.

The critical electric field values for varied thickness of PS dielectric layers are given in the supplementary information (S1). We note that the field value is about 11.1 Vμm^{-1} and corresponding dimensionless electrowetting number is $\eta = 0.14$, where $\eta = \varepsilon\varepsilon_0 U^2/2d\gamma_{LV}$. Also we have noted that subsequent EW response follows different advancing and receding paths demonstrating hysteresis as shown in Fig. 2 (b). It is worth noting that the maximum electric field we used in this study was about 20 Vμm^{-1} which is an order of magnitude below the breakdown field value (>100 Vμm^{-1}) for PS dielectric.[30] We observed consistent EW results over and over again on identically prepared PS films. The experimental findings are robust that suggest some interplay between EW induced surface modification and hysteretic EW response which is extensively analyzed in the following section.

3.2. Effects of the water-ion contact on hydrophobic polymer surfaces

The intimate contact of the water-ion on hydrophobic surfaces has been the subject of controversial debates especially for polymers like PS and other polymers having moderate glass transition temperature (T_g ~ 100 ^{o}C). Several researchers have speculated the region of reduced density at the interface between water and hydrophobic surfaces, although the nature of this depleted layer remains controversial.[36, 37] Recently, Igor *et al.*[38] have shown that degassed water could form intimate water-ions contact on PS surface resulting to the surface nano-structuration. Also the negative Zeta potential on PS surface at neutral pH indicates preferential adsorption of hydroxyl ions (OH^-) on the PS surface forming Stern layer at polymer-water interface. At Stern layer, the magnitude of ionic charge density is about few mCm^{-2} but it could generate a local electric field of about 10^7 Vm^{-1}. This electric-field is sufficiently high to reduce localized interfacial energy of the polymer surface, changing hydrodynamic equilibrium at polymer-water interface. The competition between the

electrical-surface energy and interfacial surface energy of the polymer leads to surface instability termed as electro-hydrodynamic (EHD) instability.[39] It is known that the dissolved gasses are essentially nucleated at the water-hydrophobic polymer interface in the form of surface nano-bubbles[40] which are highly stable, screening direct contact of water-ions to the polymer surface. Thus upon removal of dissolved gases increases the proximal contact of water-ions on hydrophobic polymer surface forming Stern layer that initiates EHD related surface nano-structuration.[38]

In case of EW of water droplet on PS surface, usually the applied electric field strength is in the range of 20 $V\mu m^{-1}$. This external field initiate EW of water on PS surface and also increases proximal contact of water on the polymer surface by destabilizing nano-meter thick *oil* film.[41] We conjecture that EW induced proximal contact of water-ions on polystyrene surface bring about electro-hydrodynamic (EHD) instability, following the surface nano-structuration. The nano-structuration on PS was confirmed by characterizing the morphology of pristine and electrowetted PS surfaces in detail by changing various experimental parameters like electric field, molecular weight of polystyrene, salt concentration in water and pH of water.

3.3. Surface morphology of PS

Atomic Force Microscopy was carried out *ex situ* on pristine and electrowetted PS surfaces to analyze any topological changes in the surface, after EW cycles. Fig. 4 shows AFM morphology of pristine and electrowetted PS surface, recorded after five EW cycles from two different drop-contact positions mainly at the center and along the periphery of the droplet contacts. The pristine PS surface shows root mean square (rms) surface roughness of 1.0 nm without any structuration. However, formation of hillock morphologies of varied height is clearly seen on electrowetted PS surface. The PS surface at the drop-center contact shows rms roughness value of 2.9 nm and that for the drop-peripheral contact shows rms roughness

of 2.5 nm. The rms roughness at the center of droplet contact has pronounced structuration due to uniform distribution of electric field. It is worth mentioning that this morphology possesses self-similarity on entire electrowetted surface. In addition variation in the surface roughness with PS molecular weight and magnitude of applied voltages is examined in the subsequent sections.

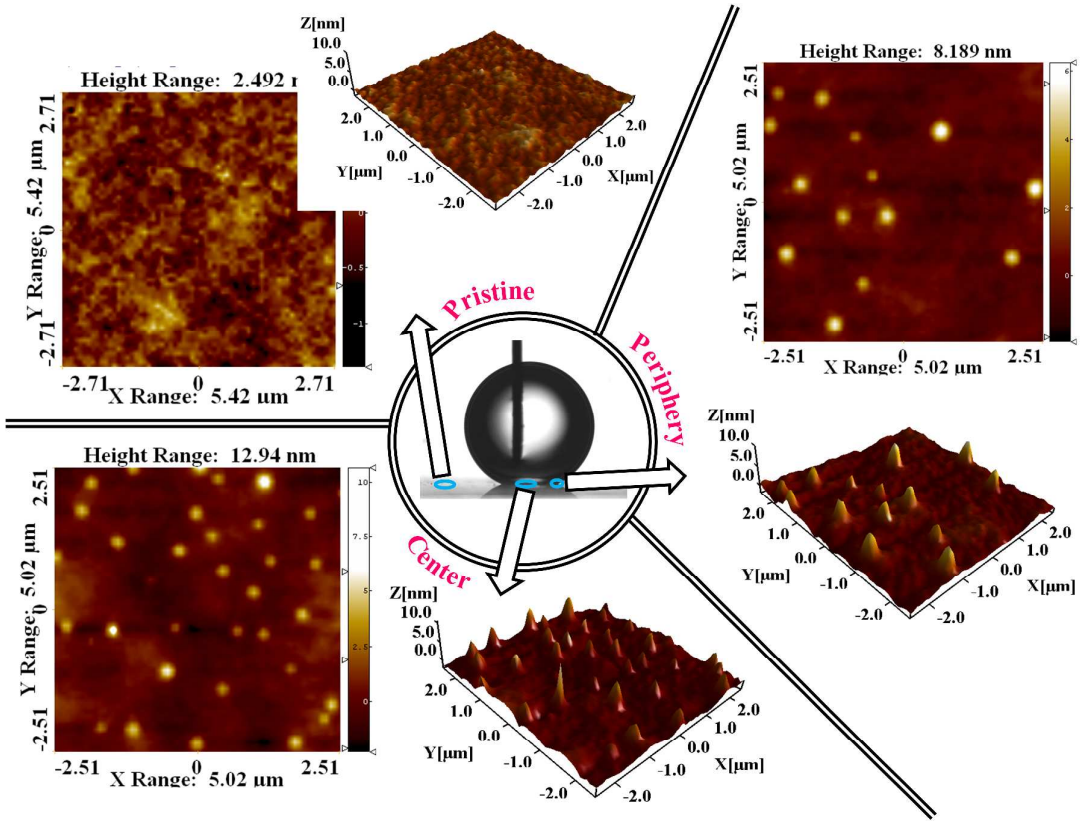

Fig. 4 AFM picture showing pristine PS surface ($\bar{M}_w$ =192000) and electrowetted surface for five voltage (EW) cycles. AFM images are shown from two different drop-contact positions mainly drop-center and along drop-periphery as indicated by arrows.

3.4. Effect of PS molecular weight on nano-structuration

The rigidity (elastic modulus) and glass transition temperature (T_g) of the polymer surface is inversely proportional to the molecular weight of PS. Thus the extent of nano-structuration due to EHD instability at polymer surface depends on the molecular weight of PS. We used

PS dielectric surfaces made from low molecular weight, $\bar{M}_W$ = 35000 (T_g = 66 °C) and high molecular weight $\bar{M}_W$ = 192000 (T_g = 86 °C). Fig. 5 shows AFM images of pristine and electrowetted PS films with varying molecular weight as mentioned above. The qualitative estimate shows that PS surface of low molecular weight ($\bar{M}_W = 35000$) after electrowetting exhibits pronounced structuration, giving rms roughness value of about 3.7 nm. Whereas electrowetted surface of high molecular weight ($\bar{M}_W = 192000$) has rms roughness value of 2.9 nm. Thus roughly the surface structuration (surface roughness) varies inversely to molecular weight which is consistent with the previous report by Igor *et al.*[42]

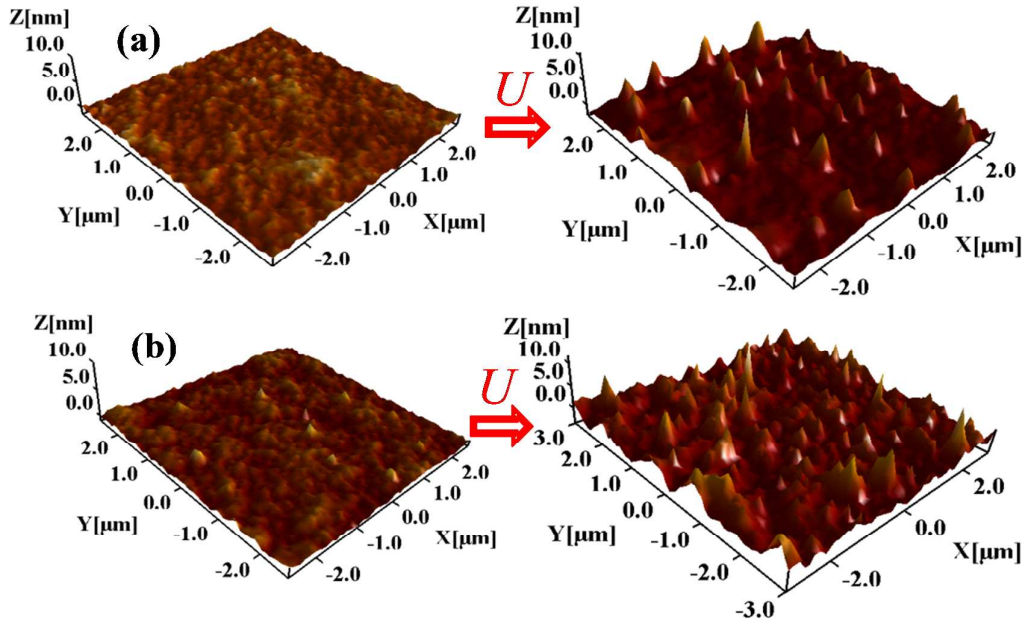

Fig. 5: AFM images of pristine and electrowetted PS surfaces of (a) $\bar{M}_W = 192000$ and (b) $\bar{M}_W =$ 35000 respectively.

3.5. Effect of external electric field on nano-structuration

It is shown in Fig. 3 that partial recovery in CA for the transient EW is observed when CA change is higher than 20° from the pristine wetting state. This change in CA is mainly brought by the external voltage. If the EW change in CA is less than 20° from its pristine

wetting angle, the partial recovery in CA is not seen. This indicates that extent of structuration could gradually increase with the voltage magnitude and planar surface may evolve into nano-structuration. To verify this possibility, we characterized PS surfaces electrowetted by varied electric field as shown in Fig. 6.

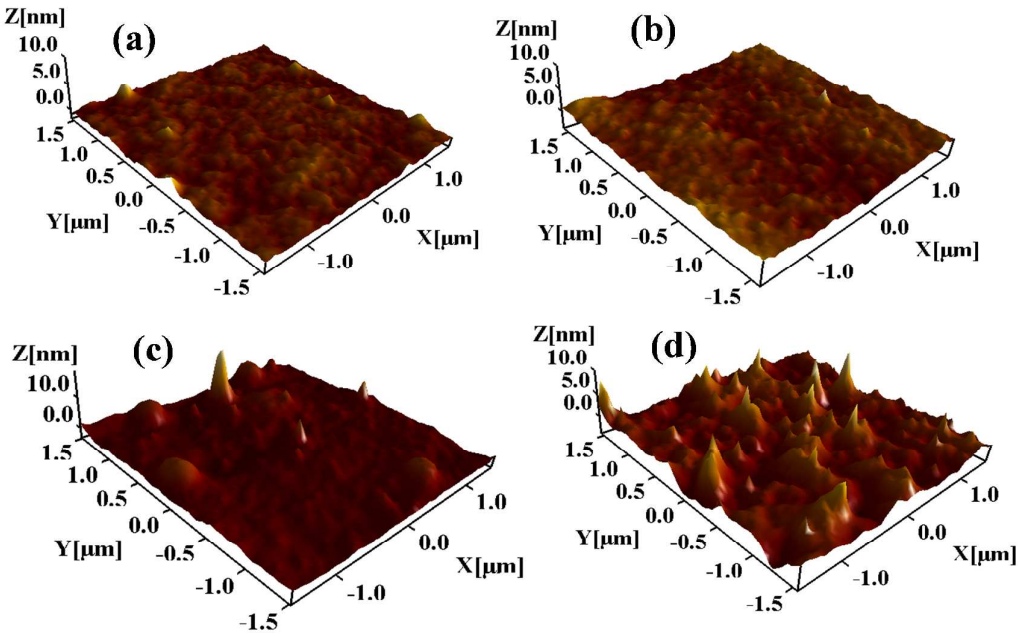

Fig. 6: AFM images of (a) pristine surface and electrowetted surface using KCl added water droplet at applied electric field of (b) 3.6 Vμm^{-1}, (c) 7.2 Vμm^{-1}, (d) 13.6 Vμm^{-1} (identical surface was prepared using PS of molecular weight $\bar{M}_W = 35000$).

Above AFM pictures clearly show the extent of nano-structuration increases with applied field. Also the nano-structuration is observed on entire surface above the applied electric field of about 13 Vμm^{-1} for PS with average molecular weight $\bar{M}_W = 35000$.

3.6. Effect of water conductivity on nano-structuration

The effect of water drop conductivity on nano-structuration is also studied to perceive any role of added KCl in water. Electrowetting was performed on distilled water and KCl added aqueous solutions having conductivity of 1 mScm^{-1} and 10 mScm^{-1}. Fig. 7 shows AFM

picture of electrowetted PS surface using water droplet of varied conductivity. It is clearly seen from these AFM images that the water conductivity does not significantly influence the nano-structuration. Also the rms surface roughness values for the electrowetted surfaces using water droplet of varied conductivity are in the same range (Fig. 7 (b-d)). It is also known that in case of DC voltage the water conductivity has no influence in quantitative changes in contact angle.

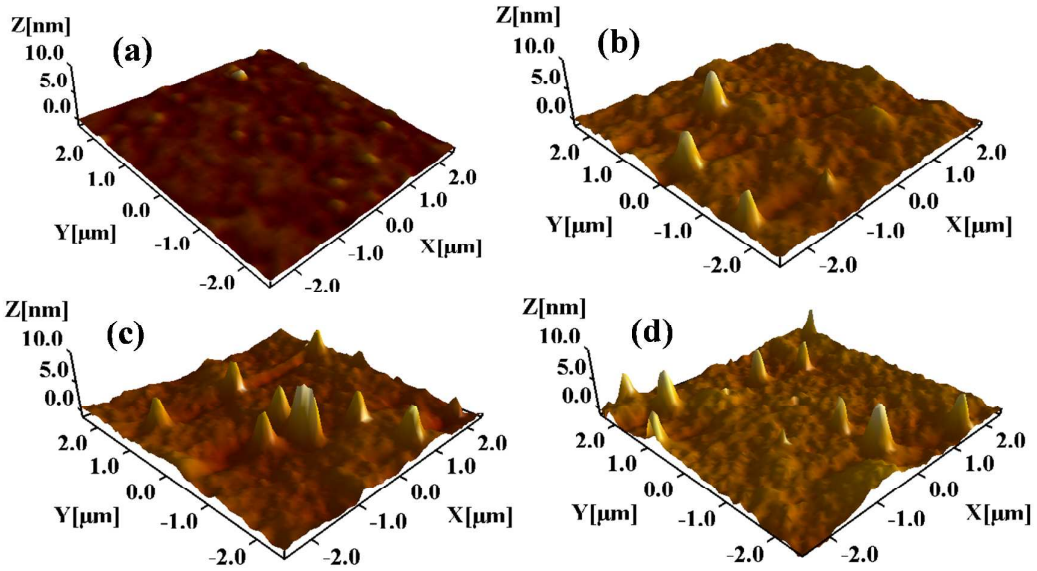

Fig. 7 AFM images of (a) pristine and electrowetted PS surface for varied droplet conductivity (b) distilled water (c) 1 $mScm^{-1}$ and (d) 10 $mScm^{-1}$. (EW was conducted on PS surface of molecular weight $\bar{M}_W = 35000$ at fixed electric field of 12 $V\mu m^{-1}$).

3.7. Effect of water pH on nano-structuration

For most of the hydrophobic polymers, the magnitude of Zeta potential increases for more basic aqueous solution (pH > 7) indicating pH dependent change in charge density at Stern layer and associated electric field across electric-double layer. To test the effect of water pH on surface structuration, EW was performed using aqueous droplet of pH 4, pH 6.5 and pH 9.2 at constant electric field and analyzed the surface morphology of post electrowetted surface. The water pH was adjusted using Merck Buffer solutions. PS surface with $\bar{M}_W =$

35000 was used and EW was carried out in ambient silicone *oil* with electric field of 12 Vμm^{-1}. Fig. 8 shows AFM images of pristine and electrowetted PS surfaces. Qualitatively, it is seen that the amount of nano-structuration on PS surface electrowetted with pH 9.2 is higher compared to that with pH 6.5 and pH 4. The rms surface roughness values for electrowetted PS surfaces are 1.5 nm, 1.9 nm and 2.2 nm for pH 4, pH 6.5 and pH 9.2 respectively. Thus water pH is crucial in the formation of nano-structuration on PS surface and is one of the controlling parameters. This reveals that the charge density at Stern layer and corresponding electric-field strength increases due to preferential adsorption of OH^- ions at the polymer surface.[43] This electric field favours EHD instability following enhanced surface nano-structurations.

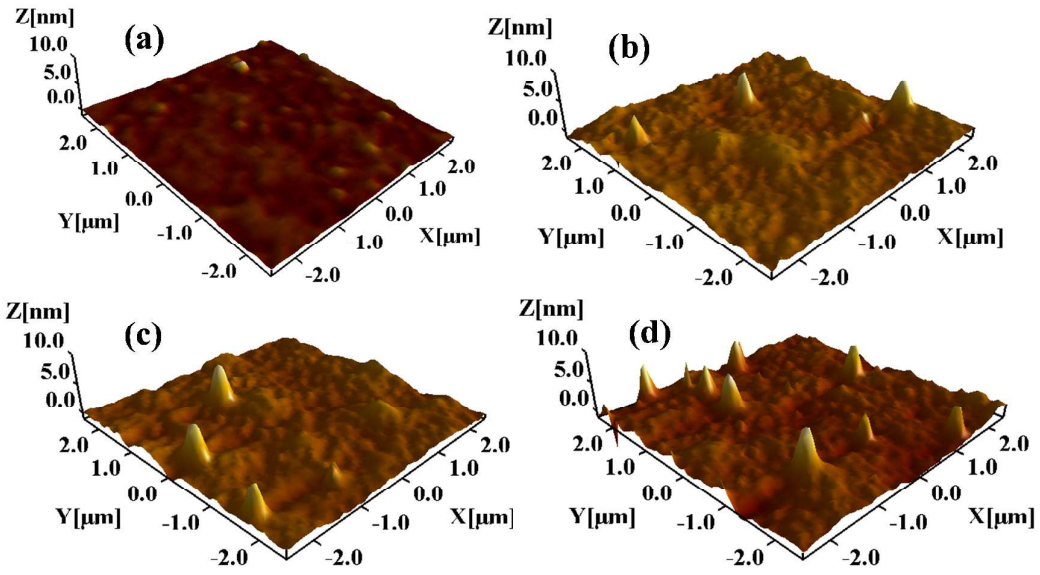

Fig. 8 AFM images of (a) pristine and electrowetted PS surface of molecular weight $\bar{M}_W = 35000$ for varied water pH of (b) pH = 4, (c) pH = 6.5 and (d) pH = 9.2 (Electric field was kept at 12 Vμm^{-1}).

Apart from the surface nano-structuration there could be chemical alternation at the surface due to the local electric field. We used ATR-FTIR spectroscopy to characterize the pristine PS surface and compared with pristine PS socked in the silicone *oil* and electrowetted PS surface. The pristine PS sample was aged in silicone oil without any EW to see any changes

in FTIR absorption due to the impregnation of silicone *oil*. Fig. 9 shows ATR -FTIR spectrum of these samples.

The FTIR absorption peaks for PS-PMMA dielectric are tabulated in the Table 1. The spectrum on pristine PS shows the prominent bands specific to aromatic vibrations of C-H bonds in the range 3001-3103 cm^{-1} (not shown in graph). Then the C-C in-plane stretching vibration of the ring can be seen at 1601cm^{-1}. Also C-H stretching and C-H bending in-plane ring vibrations are seen at 1493 cm^{-1} and 1028 cm^{-1}, respectively.

The spectrum from electrowetted PS shows considerable increase in intensity of the peak at 1028, 1069 and 1261 cm^{-1}. The peak corresponding to 1261 is assigned to C-O stretching, mainly from PMMA buffer layer. The increase in peak intensity in case of the electrowetted surface is possible due to more absorption/scattering of IR radiation from surface structuration.

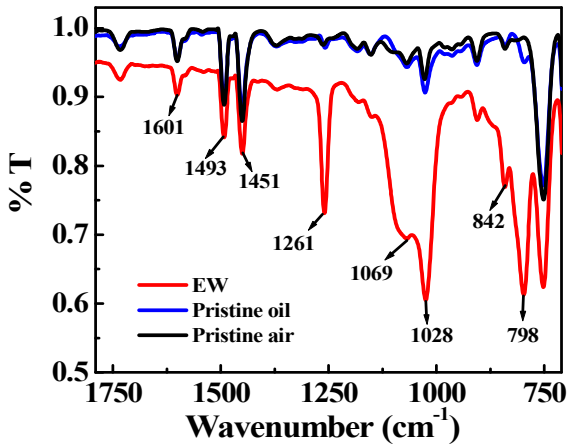

Fig. 9 ATR-FTIR spectra of polystyrene surfaces namely, pristine film (—), pristine PS aged in silicone oil (—) and Electrowetted PS surface in ambient silicone oil (—).

The peaks corresponding to 1028 and 1069 cm^{-1} are attributed to C-H in plane bending in the ring. The peak corresponding to 798 cm^{-1} is observed in the case of the PS film aged in silicone oil and is attributed to alkanes and the C-H vibrations mainly due to the impregnated

silicone oil in the PS film. The electrowetted surface does not show any new absorption peak but enhancement in the peak intensities is observed.

Table 1 ATR-FTIR spectra recorded for the pristine and electrowetted polystyrene films.

Wave number (cm^{-1})	Bond Assignment
1601	C-C in plane stretching vibration of ring
1493	C-H stretching in plane ring
1451	C-H deformation of CH_2
1261	C-O stretch
1069	C-H in plane bending in ring
1028	C-H in plane bending in ring
842	C-H out of plane bending in ring
798	Peak due to silicone oil

We have clearly shown that EW in ambient *oil* generates surface nano-structuration that leads to CAH. Also EW on PS surface in ambient *air* shows CAH[19] therefore we analyzed the surface morphology of PS films after EW cycles in *air* at relative humidity of 30 % (see the supplementary information S2). The increase in surface roughness is clearly evident due to nano-structuration. Thus EW of water drop on PS surface generates nano-structuration in ambient *oil* and in ambient *air*. It is recently shown that water flooded PS surface produces nano-structuration only in reduced ambient pressure of 10 kPa.[44] This reduction in pressure mobilizes the surface nano-bubbles hence there is intimate contact of water-ion on polymer surface as shown by Igor *et al.*[38]

We have clearly demonstrated that EW of water drop on PS surface increases proximal contact of water-ion on PS surface which is otherwise hindered due to surface nano-bubbles. The EW induced nano-structured surface offers extra pinning sites with altered interfacial energy state. This EW induced roughness acts as the surface defects at contact line[36] resulting to the hysteretic EW response. It is evident from Fig. 2 (b) that EW response follows different advancing and receding paths after the first voltage cycle. In both the cases (positive and

negative) increasing and decreasing voltage cycles show a large deviation from Young-Lippmann eqn (1) due to the nano-structuration induced hysteresis.

Several past reports have shown that nano-structuration on PS surface essentially requires either reduced pressure or degassed water to increase water-ion contact on PS surface otherwise such contacts are hindered by surface nano-bubbles.[40] Both the processes (i) water degassing and (ii) low pressure water flooding are nonlocal and cumbersome. However, EW technique does not require cumbersome vacuum pumps and degassing accessories and can be implemented on very small droplet size (< 100 μm). In the past Schaffer *et al.* demonstrated nano-structuration on PS surface, heated at 170 ^{o}C via electro-hydrodynamic (EHD) instability. The onset of the instability is seen above electric field of 100 Vμm^{-1} [45, 46] applied for time duration of about 24 hours. We have showed that EW induced nano-structuration occurs for applied electric field value of about 13 Vμm^{-1} on water droplet which is an order of magnitude less and also the EW process time is in few minutes, which is remarkably small compared to earlier reports. We have clearly demonstrated that EW based nano-structuration provides fast, on-demand and local control on nano-structuration process at room temperature.

The glass transition temperature (T_g) of supported and free standing polymer films is still a contested issue.[47, 48] Keddie *et al* performed direct measurement of T_g of PS thin films grown on hydrogen-passivated Si(111) surface.[49] The measured value of $T_g(d)$ for varied film thickness $d \leq 40$ nm were lower than the bulk value T_g (bulk). The detailed experimental results were collectively described by a simple empirical relation as: $T_g(d) = T_g(\text{bulk})\left[1 - (\alpha/d)^{\delta}\right]$, where $T_g(d)$ is measured glass transition temperature for a film of thickness d, α= 3.2 nm and exponent δ =1.8 are fit parameters obtained from the best fit to the experimental data[49]. In the present study the thickness of PS film was d=2.3 ± 0.2 μm and using above relation the value of $T_g(d)$ of PS films is almost same as T_g(bulk). Also the EW experiments

were conducted at 27 ^{o}C which is far below the glass transition temperature of PS films. Thus the formation of structuration cannot be comprehended from lowering of the value of glass transition temperatures alone.

In the recent past, several reports have shown a substantial reduction in glass transition temperature of polymer films of thickness d < 100 nm. The reduction in T_g(d < 100 nm) values was suggested to be a result of the existence of a "liquidlike" layer near the free surface of the PS film throughout the temperature range 30-150 ^{o}C. The thickness of a "liquidlike" layer increases with temperature.[50] From the present study, it is interesting to note that the extent of nano-structuration i.e. average peak-to-peak height of nano-structuration is in the range predicted by R A L Jones and co-worker.[50] Thus the existence of a "liquidlike" layer on the PS surface could lead to nano-structuration by means of EHD instability from electrowetting induced proximal contact of water-ion at room temperature.

Finally we explore the potential of the present study for enhanced loading of methylene blue dye on hydrophobic PS surface. A dilute methylene blue solution (0.5 wt. %) in distilled water was prepared for this test. A 5 μl droplet was pipetted on identically prepared PS substrates.

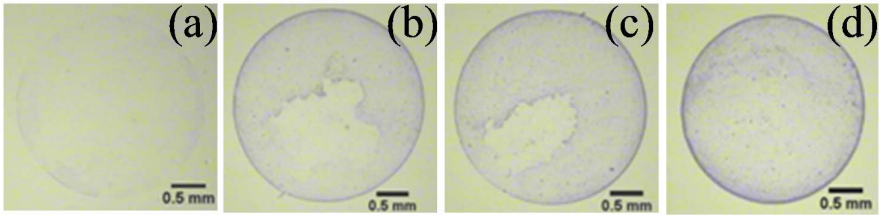

Fig. 10 Optical images demonstrate the loading of methylene blue dye on electrowetted PS surfaces ($\bar{M}_W = 192000$) for different number of voltage cycles (a) 0 (b) 2 (c) 5 (d) 10.

After EW cycle on PS surface in ambient *air*, the dye was gently removed using a lint-free tissue paper and observed under optical microscope. Fig. 10 (a-d) highlights the optical

images of the PS surface loaded with aqueous dye for the varied EW cycles. These images clearly indicate the enhanced loading of the methylene blue dye on electrowetted surface. It is seen that the dye loading increases with EW cycles and after 10 cycles it saturates. The desired value of the EW cycles for such loading mainly depends on the concentration and the electric field intensity. The process parameters can be adapted for loading of inorganic nano-particles of gold and macromolecule, bacteria etc on hydrophobic PS surface.

4. Conclusions

Electrowetting on polystyrene dielectric shows a large contact angle hysteresis of 20^{o} upon application of DC voltages, despite water droplet held in ambient silicone *oil*. This unusual effect is clearly identified with the formation of nano-structurations on PS surface in proximal contact with the water drop. The EW assisted water-ion contacts on PS surface bring *in situ* electro-hydrodynamic instability (EHD) rendering surface nano-structuration. The pronounced nano-structuration is seen on low molecular weight PS surface in comparison with high molecular weight PS, supporting EHD. It is observed that, the extent of nano-structuration increases with applied electric field and basic pH (>7). However, water conductivity due to added KCl salt does not influence the nano-structurations. Finally this method is successfully applied for the enhanced loading of a dye (methylene-blue) on the hydrophobic PS surface. The EW assisted water-ion contact offers a new possibility of targeted and on-demand wetting modification via surface nano-structurations on polystyrene surface.

Acknowledgement: AGB would like to acknowledge the financial support from BCUD, SP Pune University. YBS would like to acknowledge UGC (India) for JRF fellowship. We also acknowledge Pramod Bankar (DIAT) for assistance in AFM imaging.

References:

1. L. S. Nair and C. T. Laurencin, *Prog Polym Sci*, 2007, **32**, 762-798.
2. K. Arshak, V. Velusamy, O. Korostynska, K. Oliwa-Stasiak and C. Adley, *Ieee Sens J*, 2009, **9**, 1942-1951.
3. L. H. Chen, D. W. McBranch, H. L. Wang, R. Helgeson, F. Wudl and D. G. Whitten, *P Natl Acad Sci USA*, 1999, **96**, 12287-12292.
4. Y. K. Kang, J. Y. Wang, G. B. Yang, X. J. Xiong, X. H. Chen, L. G. Yu and P. Y. Zhang, *Appl Surf Sci*, 2011, **258**, 1008-1013.
5. P. M. van Midwoud, A. Janse, M. T. Merema, G. M. M. Groothuis and E. Verpoorte, *Anal Chem*, 2012, **84**, 3938-3944.
6. B. Bhushan, Y. C. Jung and K. Koch, *Philos T R Soc A*, 2009, **367**, 1631-1672.
7. X. Zhang, F. Shi, J. Niu, Y. G. Jiang and Z. Q. Wang, *J Mater Chem*, 2008, **18**, 621-633.
8. J. N. Lai, B. Sunderland, J. M. Xue, S. Yan, W. J. Zhao, M. Folkard, B. D. Michael and Y. G. Wang, *Appl Surf Sci*, 2006, **252**, 3375-3379.
9. K. Gotoh and S. Kikuchi, *Colloid Polym Sci*, 2005, **283**, 1356-1360.
10. M. Vallet, B. Berge and L. Vovelle, *Polymer*, 1996, **37**, 2465-2470.
11. F. Mugele and J. C. Baret, *J Phys-Condens Mat*, 2005, **17**, R705-R774.
12. B. Berge and J. Peseux, *Eur Phys J E*, 2000, **3**, 159-163.
13. R. A. Hayes and B. J. Feenstra, *Nature*, 2003, **425**, 383-385.
14. M. Hagedon, S. Yang, A. Russell and J. Heikenfeld, *Nat Commun*, 2012, **3,** 1173.
15. S. K. Cho, H. J. Moon and C. J. Kim, *J Microelectromech S*, 2003, **12**, 70-80.
16. C. S. Chen, D. N. Breslauer, J. I. Luna, A. Grimes, W. C. Chin, L. P. Leeb and M. Khine, *Lab Chip*, 2008, **8**, 622-624.
17. H. W. Li, Y. Q. Fan, R. Kodzius and I. G. Foulds, *Microsyst Technol*, 2012, **18**, 373-379.
18. N. Ktari, P. Poncet, H. Senechal, L. Malaquin, F. Kanoufi and C. Combellas, *Langmuir*, 2010, **26**, 17348-17356.
19. B. Bhushan and Y. L. Pan, *Langmuir*, 2011, **27**, 9425-9429.
20. F. Li and F. Mugele, *Appl Phys Lett*, 2008, **92**, 244108.
21. H. J. J. Verheijen and M. W. J. Prins, *Langmuir*, 1999, **15**, 6616-6620.
22. M. Vallet, M. Vallade and B. Berge, *Eur Phys J B*, 1999, **11**, 583-591.
23. E. Seyrat and R. A. Hayes, *J Appl Phys*, 2001, **90**, 1383-1386.

24. A. Quinn, R. Sedev and J. Ralston, *J Phys Chem B*, 2005, **109**, 6268-6275.
25. A. G. Papathanasiou, A. T. Papaioannou and A. G. Boudouvis, *J Appl Phys*, 2008, **103**, 034901.
26. M. Maillard, J. Legrand and B. Berge, *Langmuir*, 2009, **25**, 8368-8368.
27. R. B. Fair, *Microfluid Nanofluid*, 2007, **3**, 245-281.
28. C. Quilliet and B. Berge, *Europhys Lett*, 2002, **60**, 99-105.
29. A. G. Banpurkar, K. P. Nichols and F. Mugele, *Langmuir*, 2008, **24**, 10549-10551.
30. D. R. Lide, *ed., CRC Handbook of Chemistry and Physics, Internet Version*, 2005.
31. M. J. Santos and J. A. White, *Langmuir*, 2011, **27**, 14868-14875.
32. R. Li and Y. G. Shan, *Langmuir*, 2012, **28**, 15624-15628.
33. C. W. Extrand and S. I. Moon, *Langmuir*, 2012, **28**, 15629-15633.
34. R. E. Johnson and R. H. Dettre, *Adv. Chem. Series*, 1996, **43**, 112 and 136.
35. P.G. de Gennes, F. Brochard-Wyart, and D. Quere, *Capillary and Wetting Phenomenon: Drops, Bubbles, Pearls, Springer: New York*, 2004.
36. J. J. Kuna, K. Voitchovsky, C. Singh, H. Jiang, S. Mwenifumbo, P. K. Ghorai, M. M. Stevens, S. C. Glotzer and F. Stellacci, *Nat Mater*, 2009, **8**, 837-842.
37. D. Chandler, *Nature*, 2007, **445**, 831-832.
38. I. Siretanu, J. P. Chapel and C. Drummond, *Acs Nano*, 2011, **5**, 2939-2947.
39. N. Wu and W. B. Russel, *Nano Today*, 2009, **4**, 180-192.
40. M. A. J. van Limbeek and J. R. T. Seddon, *Langmuir*, 2011, **27**, 8694-8699.
41. A. Staicu and F. Mugele, *Phys Rev Lett*, 2006, **97**, 167801.
42. I. Siretanu, J. P. Chapel and C. Drummond, *Macromolecules*, 2012, **45**, 1001-1005.
43. L. S. McCarty and G. M. Whitesides, *Angew Chem Int Edit*, 2008, **47**, 2188-2207.
44. H. Tarábková, Z. Bastl and P. Janda, *Langmuir*, 2014, **30**, 14522–14531.
45. E. Schaffer, T. Thurn-Albrecht, T. P. Russell and U. Steiner, *Nature*, 2000, **403**, 874-877.
46. M. D. Morariu, N. E. Voicu, E. Schaffer, Z. Q. Lin, T. P. Russell and U. Steiner, *Nat Mater*, 2003, **2**, 48-52.
47. J. A. Forrest, K. DalnokiVeress, J. R. Stevens and J. R. Dutcher, *Phys Rev Lett*, 1996, **77**, 2002-2005.
48. C. B. Roth and J. R. Dutcher, *J Electroanal Chem*, 2005, **584**, 13-22.
49. J. L. Keddie, R. A. L. Jones and R. A. Cory, *Europhys Lett*, 1994, **27**, 59-64.
50. S. Kawana and R. A. L. Jones, *Phys Rev E*, 2001, **63**, 021501.

TOC

Electrowetting of water droplet on polystyrene dielectric generates surface nano-structuration by means of electrohydrodynamic instability via intimate water-ion contacts.